

# Nanoparticles Sustain Expression of Flt Intracellular Receptors in the Cornea and Inhibit Injury-Induced Corneal Angiogenesis

Pooja D. Jani,<sup>1,2</sup> Nirbhaj Singh,<sup>1,2</sup> Crystal Jenkins,<sup>1</sup> Swita Raghava,<sup>3</sup> Yun Mo,<sup>3</sup> Shivan Amin,<sup>1</sup> Uday B. Kompella,<sup>3</sup> and Balamurali K. Ambati<sup>1</sup>

**PURPOSE.** To determine whether long-term expression of intracellular receptors can be achieved using plasmid albumin nanoparticles and whether nanoparticles can inhibit and cause regression of murine corneal neovascularization induced by mechanical-chemical trauma.

**METHODS.** Albumin nanoparticles encapsulating pCMV.Flt23K were developed as a lyophilized product that is easily redispersed in an aqueous medium. Nanoparticles were injected into the corneas of uninjured BALB/c mice and observed for toxicity for 3 weeks. Entry of nanoparticles into corneal cells was demonstrated through transmission electron microscopy and confocal imaging. Naked pCMV.Flt23K, nanoparticles encapsulating pCMV.Flt23K, or empty pCMV nanoparticles were injected into uninjured mouse corneas. These corneas were subjected to mechanical alkali trauma 3 weeks after injection.

**RESULTS.** Nanoparticles were nontoxic to the cornea and entered into corneal keratocyte cytoplasm. They persisted for at least 4 weeks in the cornea, expressed effective intracellular receptor levels for at least 5 weeks, and reduced corneal neovascularization by approximately 40% ( $P = 0.035$ ) at 5 weeks after administration.

**CONCLUSIONS.** Albumin nanoparticles are not toxic to the cornea and can express intracellular receptors for extended periods that are effective in suppressing injury-induced corneal neovascularization. (*Invest Ophthalmol Vis Sci.* 2007;48:2030–2036) DOI:10.1167/iovs.06-0853

Angiogenesis, the growth of new blood vessels, is a fundamental biological process that plays a central role in the pathogenesis of cancer, diabetic retinopathy, and macular degeneration. VEGF (vascular endothelial growth factor) promotes vascular endothelial cell migration, proliferation,

inhibition of apoptosis, vasodilation, and increased vascular permeability. In the cornea, the angiogenic process has been shown to be driven by increased secretion of VEGF.<sup>1</sup> VEGF transcription is amplified in response to oncogenes, hypoxia, and other insults. Strategies to inhibit VEGF action have included VEGF receptors with blocking antibodies, decoy receptors for VEGF, and anti-VEGF antibodies.<sup>2–5</sup> These strategies have generally reduced neovascularization by only 30% to 50%.<sup>6–9</sup>

We believe it important to target VEGF intracellularly, as several cell types respond to their own VEGF production in an autocrine fashion. VEGF autocrine loops have also been demonstrated in endothelial cells and cancer cells,<sup>10–15</sup> including in hypoxic human vascular endothelial cells (HUVECs).<sup>11</sup> Further, VEGF can upregulate its own receptor, VEGFR-2.<sup>12,13,15</sup>

Flt, or VEGF receptor 1, consists of seven domains and has the highest affinity for VEGF. Domain deletion studies have shown that domain 1 serves as a secretion signal, and domains 2 to 3 are the key binding regions for VEGF.<sup>16–18</sup> KDEL is a quadriptide retention signal (Lys-Asp-Glu-Leu) that binds endoplasmic reticulum retention receptors,<sup>14</sup> preventing the secretion of ligands of proteins that are coupled to KDEL. Linkage of KDEL to various proteins (creation of “intrakines”) reduces the expression of cognate receptors with significant roles in different diseases. Coupling stromal derived factor (SDF) with KDEL blocks cell surface expression of SDF’s receptor, CXCR-4. Similar efforts have been used to downregulate cell surface expression of other receptors, including CCR-5 and the interleukin-4 receptor.<sup>19–21</sup>

In this study, a long-term delivery approach was introduced for antiangiogenic therapy, via nanoparticles carrying plasmids that express Flt intracellular receptors. We decided to investigate whether albumin nanoparticles containing VEGF-intracellular receptors would afford the desired long-term delivery of the KDEL product. Albumin nanoparticles are biodegradable polymers and allow encapsulation of drugs in a sustained fashion. It is a common serum protein that is biodegradable and has been used as a substrate for delivering chemotherapy encapsulated in nanoparticles (Abraxane; Abraxis BioScience, Los Angeles, CA). Nanoparticles range in size from 1 to 1000 nm and have been shown to deliver drugs (e.g., oligonucleotides, budesonide) to retinal pigmented epithelial cells in vitro, and in vivo to the retina, lens, vitreous, and cornea after subconjunctival injection.<sup>22,23</sup> It has been determined that 200-nm particles are retained for at least 2 months in the periocular space,<sup>23</sup> and this size will be used to ensure particle retention in the cornea.

In this study, albumin nanoparticles encapsulating pCMV.Flt23K were developed and injected into mouse corneas. We hypothesized that plasmid albumin nanoparticles when administered well before corneal injury would persist in the confined stromal space and express Flt intracellular receptors in a prolonged manner to inhibit murine corneal neovascularization induced by mechanical chemical trauma.

Therefore, we tested the long-term effectiveness of nanoparticles expressing intracellular receptors by delivering them well be-

From the <sup>1</sup>Department of Ophthalmology, Medical College of Georgia, Augusta, Georgia; and the <sup>3</sup>Department of Pharmaceutical Sciences, University of Nebraska Medical Center, Omaha, Nebraska.

<sup>2</sup>Contributed equally to the work and therefore should be considered equivalent authors.

The plasmids and delivery system presented herein are included in provisional patent applications filed with the United States Patent Office.

Supported by the Knights-Templar Eye Foundation (BKA) and National Eye Institute Grant R24EY017045 (UBK, through Emory University). SR is the recipient of a graduate student fellowship at UNMC.

Submitted for publication July 24, 2006; revised October 26, 2006; accepted March 12, 2007.

Disclosure: P.D. Jani, None; N. Singh (P); C. Jenkins, None; S. Raghava, None; Y. Mo, None; S. Amin (P); U.B. Kompella (P); B.K. Ambati (P)

The publication costs of this article were defrayed in part by page charge payment. This article must therefore be marked “advertisement” in accordance with 18 U.S.C. §1734 solely to indicate this fact.

Corresponding author: Balamurali K. Ambati, Medical College of Georgia, Department of Ophthalmology, 1120 15th Street, CB1611, Augusta, GA 30912; bambati@mail.mcg.edu.

fore corneal injury and observing over an extended period, to assess whether this approach can more sustainably prevent neovascularization than a short-duration intervention, such as naked plasmid delivery.

## METHODS

All experiments were conducted in accordance with the ARVO Statement for the Use of Animals in Ophthalmic and Vision Research.

### Synthesis of KDEL Constructs

cDNA encoding domains 2 and 3 of Flt (the binding domains for VEGF) were amplified from a corneal cDNA library (Open Biosystems, Huntsville, AL). Primers encoding 3' KDEL were then used to generate the Flt23K construct<sup>24</sup> (predicted size of 667 bp). cDNA clones had restriction sites of 5' *Bam*HI and 3' *Eco*RI. These were digested and ligated into the pCMV Script vector (Stratagene, La Jolla, CA) with neomycin resistance. *Escherichia coli* DH5  $\alpha$  cells were transformed with these at a ratio of 6 to 1, and colonies grown in neomycin-agar medium were miniprepmed to isolate pCMV.Flt23K.

### Development of Nanoparticles

**Plasmid Nanoparticle Formulation.** Human serum albumin (HSA) nanoparticles containing Flt23K plasmid were prepared by a coacervation process followed by a cross-linking step using glutaraldehyde.<sup>25</sup> Briefly, a 2% wt/vol solution of HSA was incubated with Flt23K plasmid solution in tris-EDTA buffer equivalent to 5  $\mu$ g plasmid/mg albumin, for 1 hour on ice. This aqueous phase was then desolvated by drop-wise addition into ethanol equivalent to double the volume of aqueous phase, under continuous stirring. The coacervates formed were hardened by the addition of glutaraldehyde albumin. The resultant nanoparticles were separated by ultracentrifugation at 20,000 rpm for 45 minutes. The nanoparticle pellet was resuspended in 10 mL mannitol solution (2% wt/vol) and lyophilized to obtain the dried product. FITC-labeled HSA nanoparticles were prepared by incorporating 10% wt/wt of FITC-labeled HSA in the aqueous phase along with unlabeled albumin, and performing nanoparticle synthesis in a manner similar to that just described.

**Nanoparticle Size and Morphology Analysis.** The particle size and the  $\zeta$  potential were measured with a  $\zeta$ -potential analyzer (Zeta Plus; Brookhaven Instruments Ltd., Holtsville, NY), which employs the dynamic light-scattering technique for particle size measurement. The particle size and  $\zeta$ -potential measurements were performed after a 1:1000 dilution of particle stock before lyophilization in filtered deionized water.

The particle morphology was studied using transmission electron microscopy (TEM). Initially, carbon-coated grids were floated on a droplet of the nanoparticle suspension on a flexible plastic film (Parafilm; Pechiney Plastic Packaging, Neenah, WI), to permit the adsorption of the nanoparticles onto the grid. After the grid was blotted with a filter paper and air dried for 5 minutes, it was transferred onto a drop of the negative stain. Next, the grid was blotted with a filter paper and air dried for 5 minutes. Vanadium (NanoVan; Nanoprobes, Stony Brook, NY) was used as a negative stain. Finally, the samples were examined with an electron microscope set at 80 kV (410LS; Phillips, FEI Co., Hillsboro, OR).

**Plasmid Loading.** The plasmid loading was determined by digesting 5 mg of the lyophilized product in 5 mL 0.1 N NaOH. The protein was precipitated by the addition of 10% vol/vol trichloroacetic acid (TCA), and the precipitate was spun down by centrifugation at 10,000 rpm for 15 minutes. The absorbance of supernatant at 260 nm was used to determine plasmid content.

### Corneal Intrastromal Injection

Effective transfection of plasmid delivery to the cornea has been described.<sup>26</sup> Under direct microscopic observation, a nick in the epi-

thelium and anterior stroma of a (BALB/c) mouse cornea was made in the midperiphery with a 0.5-in., 30-gauge needle (BD Biosciences, Franklin Lakes, NJ). A 0.5-in., 33-gauge needle with a 30° bevel on a 10- $\mu$ L gas-tight syringe (Hamilton, Reno, NV) was introduced into the corneal stroma and advanced 1.5 mm to the corneal center. Two microliters of plasmid solution was forcibly injected into the stroma, to separate the corneal lamellae and disperse the plasmid.

To determine whether nanoparticles are toxic to the cornea, we resuspended the nanoparticles to achieve a concentration of 1  $\mu$ g of plasmid per 1  $\mu$ L of PBS, and injected 2  $\mu$ L of this suspension (conventional and pCMV.Flt23K-loaded albumin nanoparticles) into corneas of uninjured BALB/c mice ( $n = 7$  for each) and observed the corneas for toxicity weekly for 3 weeks.

### Mechanical Alkali Trauma Model of Corneal Neovascularization

Topical proparacaine and 2  $\mu$ L of 1 M NaOH were applied to both corneas of each mouse. The corneal and limbal epithelia were removed with a Tooke corneal knife (Katena Products, Denville, NJ) in a rotary motion parallel to the limbus. Topical erythromycin ophthalmic ointment was instilled immediately after epithelial denudation.

To determine whether nanoparticles encapsulating pCMV.Flt23K are effective at inhibiting corneal neovascularization on a long-term basis, mouse corneas were injected with albumin nanoparticles loaded with pCMV.Flt23K, empty pCMV, or naked pCMV.Flt23K. The nanoparticles were resuspended to achieve a concentration of 1  $\mu$ g of plasmid per 1  $\mu$ L of PBS, and 2  $\mu$ L of this suspension was injected into the corneas of uninjured BALB/c mice ( $n = 7$  for each). Three weeks after injection, these corneas underwent mechanical alkali trauma and were photographed at 7 and 14 days after the trauma. This time frame was chosen because our prior investigations<sup>24</sup> demonstrated the effectiveness of intracorneal nanoparticles expressed by naked plasmids in inhibiting injury-induced neovascularization for 1 to 2 weeks after injection. We therefore designed this study's experiments to assess the effectiveness of nanoparticle-delivered plasmids expressing intracorneal nanoparticles in inhibiting angiogenesis out to 5 weeks after injection.

### Electron Microscopy

To demonstrate entry and retention of nanoparticles into corneal cells, we photographed nanoparticle-injected mouse corneas by TEM and two-photon microscopy over a 3-week period.

After intracorneal injection, the corneas were enucleated and fixed in a mixture of 2% glutaraldehyde, 2% formaldehyde, and 0.5% acrolein. The corneas were isolated and sectioned at the site of injection. The sections were imaged with a transmission electron microscope set at 80 kV (410LS; Phillips, FEI Co.).

### Two-Photon Microscopy

A laser scanning microscope (LSM 510META; Carl Zeiss Meditec, Inc., Thornwood, NY) and laser system (MIRA 900; Coherent, Santa Clara, CA) were used to perform two-photon microscopy on freshly enucleated mouse corneas. The corneas were placed on slides with a coverslip. Each cornea was surrounded by PBS in a well of vacuum grease.

### Labeling of Corneal Keratocytes

For assessment of whether fluorescent nanoparticles colocalize with keratocyte cell bodies, the corneas were harvested 1 week after injection with FITC-conjugated nanoparticles. The corneas underwent cryosectioning and staining with propidium iodide (1:5000 dilution) for 1 minute, followed by washing and mounting with a coverslip.

### Labeling of Corneal Neovascularization

Immunohistochemical staining for vascular endothelial cells was performed on corneal flatmounts. Fresh corneas were dissected, rinsed in PBS for 30 minutes, and fixed in 100% acetone (Sigma-Aldrich, St. Louis, MO) for 20 minutes. After the corneas were washed in PBS,

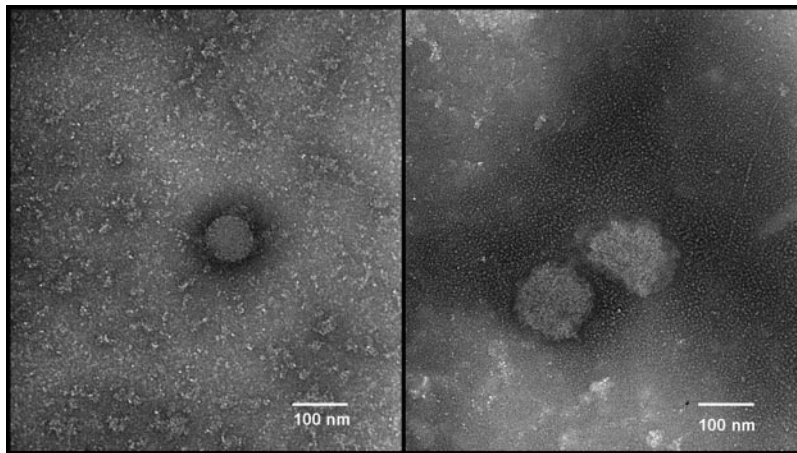


**FIGURE 1.** TEM micrographs of HSA nanoparticles. (A) Blank HSA nanoparticles; (B) plasmid-loaded nanoparticles. Magnification,  $\times 153,000$ .

nonspecific binding was blocked with 0.1 M PBS and 2% albumin (Sigma-Aldrich) for 1 hour at room temperature. Incubation with FITC-coupled monoclonal anti-mouse CD31 antibody (BD-PharMingen, San Diego, CA) at a concentration of 1:500 in 0.1 M PBS and 2% albumin at 4°C overnight was followed by subsequent washes in PBS at room temperature. The corneas were mounted with an antifading agent (Gelmount; Biomedica, Inc, San Francisco, CA) and visualized with a fluorescence microscope (Leica, Wetzlar, Germany).

### Quantification of Corneal Neovascularization

Digital quantification of corneal neovascularization has been described.<sup>27</sup> Images of the corneal vasculature were captured with a CD-330 charge-coupled device (CCD) camera (Dage-MIT, Inc., Michigan City, IN) attached to a fluorescence microscope (MZ FLIII; Leica Microsystems Inc., Deerfield, IL). The images were analyzed on a computer with commercial software (OpenLab; Improvion Inc., Lexington, MA), resolved at  $624 \times 480$  pixels, and converted to tagged information file format (TIFF) files. The neovascularization was quantified by setting a threshold level of fluorescence above which only vessels were captured. The entire mounted cornea was analyzed to minimize sampling bias. The quantification of the neovascularization was performed in masked fashion. The total corneal area was outlined, with the innermost vessel of the limbal arcade used as the border. The total area of neovascularization was then normalized to the total corneal area, and the percentage of the cornea covered by vessels was calculated.

### Cell Fractionation

The localization of Flt23K in the endoplasmic reticulum was confirmed by organelle fractionation assay with a cell compartment kit (Qproteome; Qiagen, Valencia, CA) according to the manufacturer's instructions. Briefly, mice corneas were harvested, freeze fractured with a mortar and pestle, and then suspended in 1 mL of ice-cold extraction buffer CE1. They were then incubated on ice for 10 minutes. The lysate was centrifuged at 1000g for 10 minutes, and the pellet was suspended in 1 mL of the extraction buffer CE2. The samples were then incubated for 30 minutes on ice. After the incubation, the suspensions were

centrifuged at 6000g for 10 minutes, and the supernatant was recovered. This fractionation primarily contains the proteins from the endoplasmic reticulum and was used for Western blot analyses.

### Western Blot Analysis

Western blot analysis of corneas transfected with pCMV.Flt23K first involved freeze-fracturing with a mortar and pestle and placement in 200  $\mu$ L RIPA buffer (Tris-HCl, NaCl, NP-40, Na-deoxycholate, and protease inhibitors). After incubation in RIPA buffer for 1 hour, the samples were sonicated on ice four times at 15-second intervals and level-4 intensity. The corneal lysates and corneal cell fractions were then loaded onto 10% SDS-PAGE gels. Nitrocellulose paper (NCP) membranes were probed for Flt (expected mass of Flt23K construct, 23 kDa) in a dilution of 1:1000 Flt primary antibody. Ten percent milk and 1:1000 of the appropriate secondary antibody (Abcam, Cambridge,

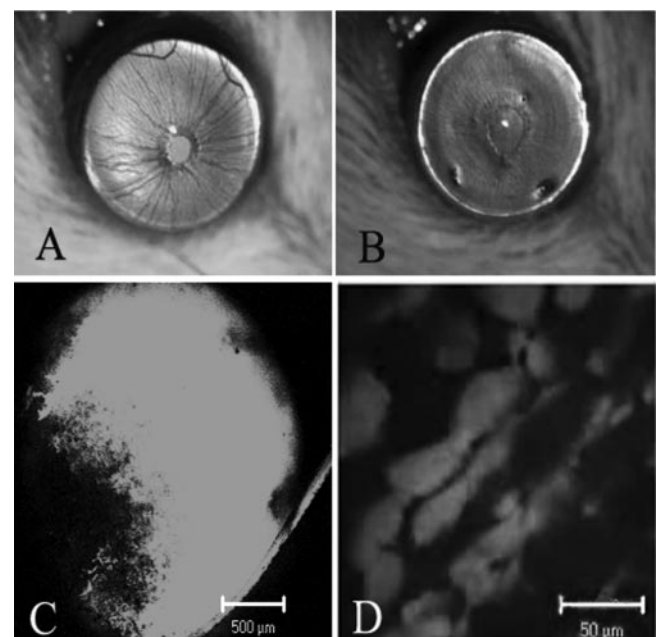


**FIGURE 2.** (A, B) Representative photographs of mouse corneas injected with conventional (A) or pCMV.Flt23K-containing (B) nanoparticles. Corneas remained clear throughout the 3-week observation period without evidence of toxicity. The iris remains fully visible in these photographs, as the corneas were translucent. Fluorescence-labeled nanoparticles were present throughout the injected cornea (C), with cytoplasmic fluorescence visible at higher magnification (D). Magnifications: (C)  $\times 5$ ; (D)  $\times 40$ .

**TABLE 1.** Physical Characteristics of Human Serum Albumin Nanoparticles

Particle Type	Effective Diameter (nm)	Polydispersity	$\zeta$ Potential (mV)
Blank albumin	$147.6 \pm 3.5$	$0.295 \pm 0.008$	$-20.38 \pm 0.98$
Plasmid albumin	$156.2 \pm 1.8$	$0.154 \pm 0.016$	$-21.06 \pm 2.43$
FITC albumin	$140.0 \pm 1.7$	$0.194 \pm 0.004$	$-21.08 \pm 3.24$

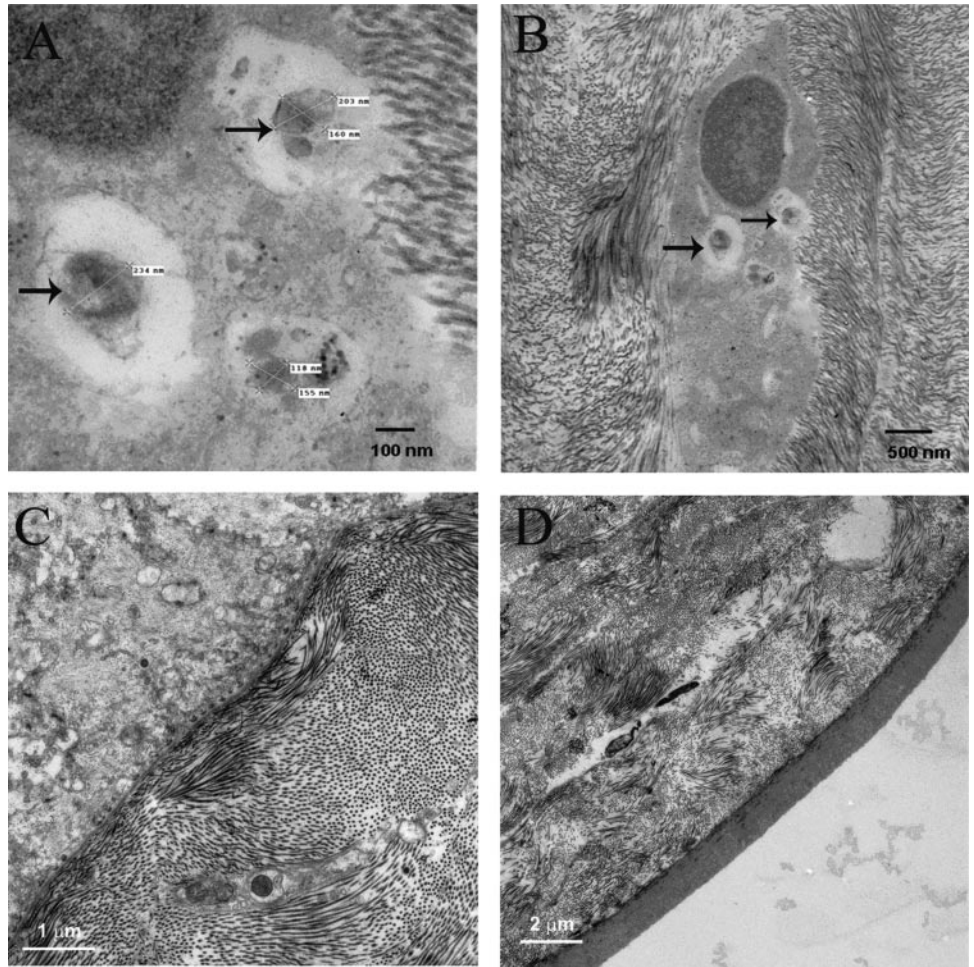


**FIGURE 3.** (A, B) TEM confirmed that nanoparticles were taken up into the corneal keratocyte cytoplasm. (C, D) Negative control. *Arrows:* nanoparticles. Magnification: (A, B)  $\times 82,000$ ; (C)  $\times 5,000$ ; (D)  $\times 2,000$ .

MA) was used to incubate the membranes for 2 hours at room temperature. After they were washed with PBS-Tween 20, the membranes were developed (BioMax Light Film; Eastman Kodak, Rochester, NY) with a chemiluminescence kit (ECL; Pierce, Rockford, IL).

**Statistics**

Statistical analysis was performed (SPSS for Windows; SPSS, Inc., Chicago, IL), and the data were analyzed by independent-sample Student's *t*-test. A type I error not exceeding 0.05 was deemed significant.

**RESULTS**

**Nanoparticle Toxicity and Morphology**

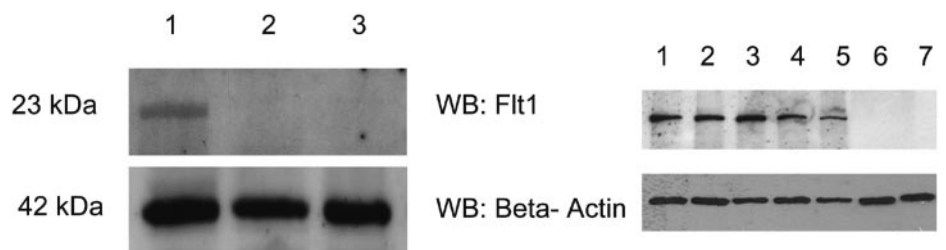
TEM images of nanoparticles demonstrated a spherical particle morphology (Fig. 1). Physical characteristics of the nanopar-

ticles are listed in Table 1. After injection of nanoparticles into the cornea, we found no evidence of inflammation, edema, opacification, or other toxicity to the corneas, and the corneas remained transparent (Fig. 2). Two-photon microscopy of corneas injected with fluorescence-labeled nanoparticles showed the presence of nanoparticles in the corneal keratocytes. Cytoplasmic fluorescence was visible at high magnification ( $40\times$ ) (Fig. 2). Transmission electron microscopy revealed that nanoparticles entered the corneal keratocyte cytoplasm (Fig. 3).

**Expression and Release of Nanoparticles in the Cornea**

Organelle fractionation confirmed the localization of Flt23K (expected molecular mass, 23 kDa) in the endoplasmic reticulum (Fig. 4). Next, we injected pCMV.Flt23K and nanopar-

**FIGURE 4.** Representative Western blot analyses of Flt23K expression. *Left:* Flt23K was expressed in the endoplasmic reticular fraction of mouse corneas (lane 1) but not in the cytosolic fraction (lane 2) or in corneas transfected with empty pCMV (lane 3). *Right:* Flt23K was expressed at 4 (lane 1) and 8 (lane 2) days after injection of pCMV.Flt23K into the cornea. Flt23K was expressed at 1 (lane 3), 3 (lane 4), and 5 (lane 5) weeks after injection of nanoparticles loaded with pCMV.Flt23K. No Flt23K expression was observed 1 week after injection with empty pCMV (lane 6) or nanoparticles loaded with empty pCMV (lane 7).



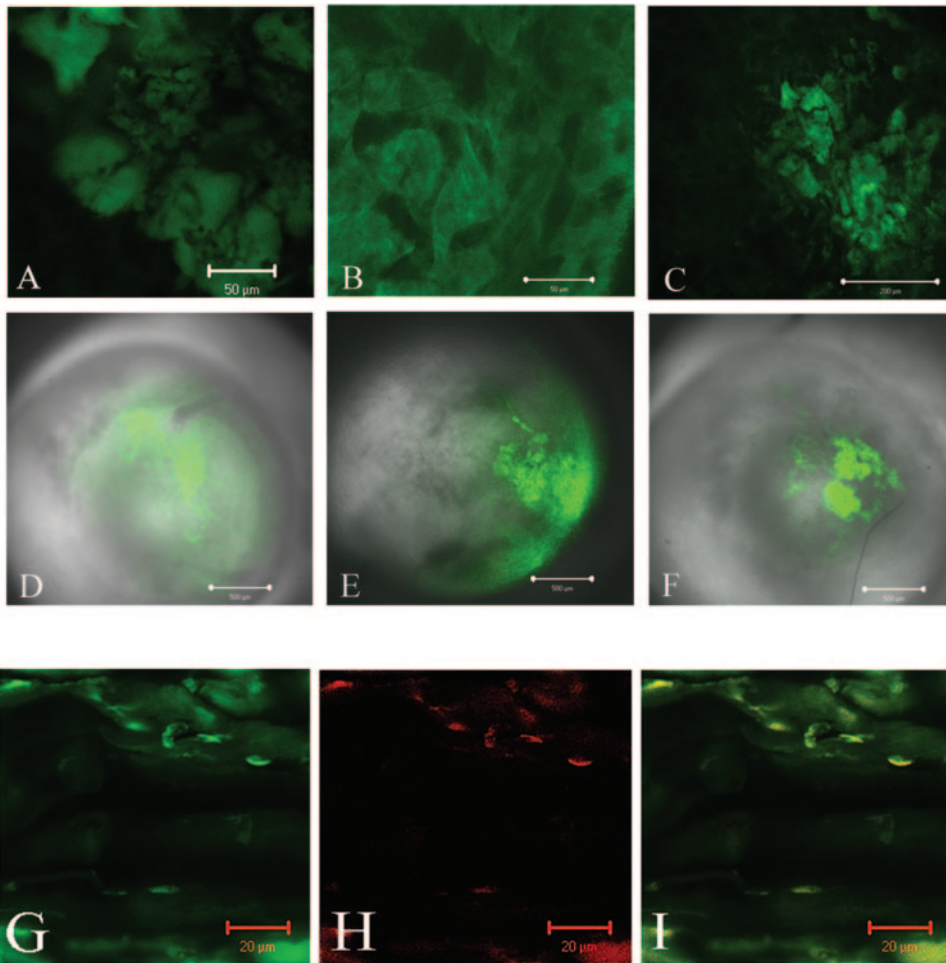


**FIGURE 5.** FITC-conjugated nanoparticles were expressed in corneal keratocytes. (A, D) One week after injection; (B, E) 2 weeks after injection; (C, F) 4 weeks after injection. (G) Fluorescence observed within corneal keratocytes 1 week after FITC-conjugated nanoparticle injection; (H) propidium iodide labeling of keratocytes; (I) merger of images in (G) and (H). Magnification: (A, B)  $\times 40$ ; (C)  $\times 20$ ; (D-F)  $\times 5$ ; (G-I)  $\times 63$ .

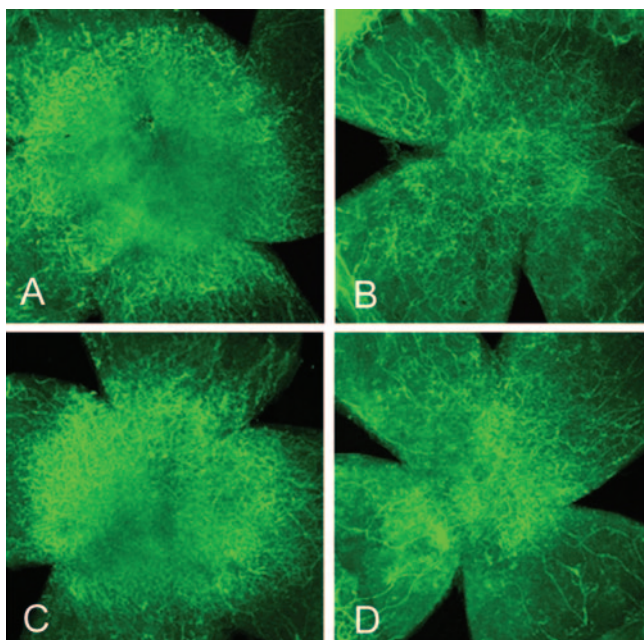


**FIGURE 6.** Representative photographs of corneas treated with pCMV.Flt23K-loaded nanoparticles (A), naked pCMV.Flt23K (B), empty pCMV (C), or saline (D), 3 weeks before corneal injury. Eyes were harvested 2 weeks after corneal injury. Neovessels were stained with anti-CD31 antibody.

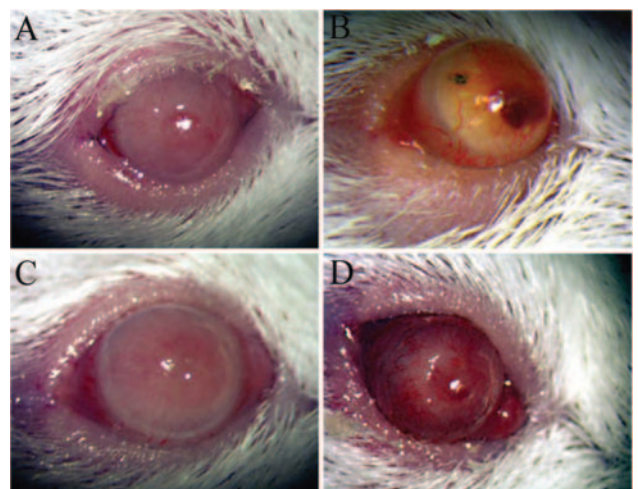


**FIGURE 7.** Representative color photographs of mouse corneas injected with nanoparticles expressing pCMV.Flt23K (A, C), naked pCMV.Flt23K (B), or nanoparticles expressing empty pCMV (D). Three weeks after injection, corneas were injured, and photographs were taken 2 weeks after injury. pCMV.Flt23K-loaded nanoparticles successfully inhibited injury-induced neovascularization even when injected long before injury, unlike naked pCMV.Flt23K and nanoparticles loaded with empty pCMV.

## Flt23K-loaded nanoparticles inhibit corneal NV

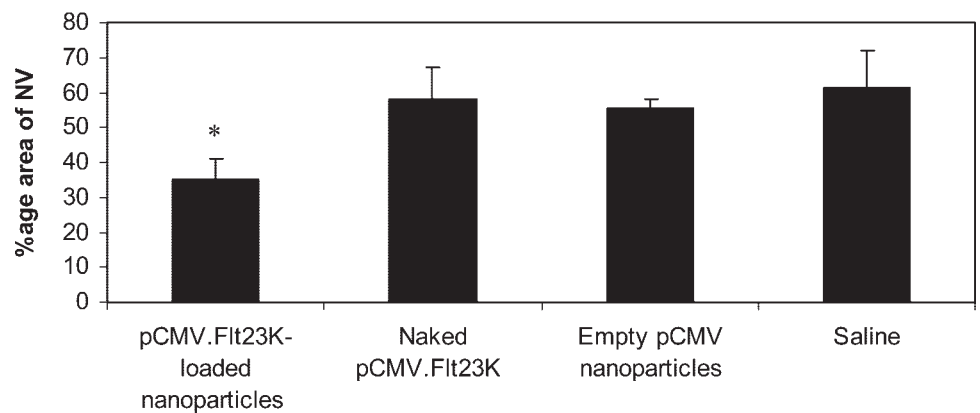


**FIGURE 8.** Quantitative data of corneas treated with pCMV.Flt23K-loaded nanoparticles, naked pCMV.Flt23K, empty pCMV, or saline 3 weeks before corneal injury. Eyes were harvested 2 weeks after corneal injury.  $n = 7$  per group.

ticles loaded with pCMV.Flt23K into the mouse corneas (empty pCMV and blank nanoparticles loaded with empty pCMV served as control specimens). Flt23K was expressed by the naked plasmids in the corneas for 8 days and by the nanoparticles for 5 weeks (Fig. 4). FITC-conjugated nanoparticles were injected into the cornea, and fluorescence was observed for 4 weeks (Fig. 5). Colocalization of fluorescence to cell bodies in keratocytes was confirmed by propidium iodide staining (Fig. 5).

### Effect of Nanoparticles Expressing Intracorneal Inhibitors on Corneal Neovascularization

Mouse corneas injected with pCMV.Flt23K-loaded nanoparticles 3 weeks before mechanical alkali trauma showed a mean percentage of corneal neovascularization of  $35.0\% \pm 6.0\%$  2 weeks after injury. This period was less than in mouse corneas that had been injected 3 weeks before injury with naked pCMV.Flt23K ( $58.3\% \pm 8.7\%$ ), empty pCMV nanoparticles ( $55.4\% \pm 2.7\%$ ), or saline ( $61.6\% \pm 10.5\%$ ; for all,  $P < 0.05$ ;  $n = 7$ ; Figs. 6–8). There were no statistically significant differences among corneas injected with saline, naked plasmid, or empty nanoparticles.

## DISCUSSION

Our previous work with a clinically relevant model of corneal neovascularization demonstrated that the use of sodium hydroxide epithelial denudation followed by mechanical scraping consistently induces  $360^\circ$  of neovascularization<sup>28</sup> driven by VEGF.<sup>29</sup> We have shown that angiostatin and genetic ablation of CCR2 and CCR5 can partially inhibit corneal neovascularization<sup>28,30,31</sup> in this model.

We have also demonstrated that Flt intracorneal inhibitors can inhibit VEGF expression by corneal cells *in vitro* and inhibit injury-induced corneal angiogenesis *in vivo*.<sup>24</sup> Flt intracorneal inhibitors encoding Flt23K (domains 2–3 of Flt coupled with KDEL) inhibit corneal neovascularization induced by mechanical alkali trauma.<sup>24</sup> Delivering intracorneal inhibitors (with a 33-gauge microsyringe needle [Hamilton]) can suppress hypoxia-induced VEGF secretion in human corneal epithelial (HCE) cells, injury-induced VEGF secretion, leukocyte infiltration, and corneal angiogenesis.

In this study, nanoparticles delivered plasmids expressing intracorneal inhibitors for extended periods and inhibited injury-induced corneal neovascularization long after the time of injection. Furthermore, the nanoparticles were not toxic to the cornea and are taken up by corneal keratocytes. To our knowledge,

this is the first evidence of long-term efficacy of gene delivery by nanoparticles in the cornea.

Drug delivery of potential intraocular therapies against angiogenesis is bedeviled by a potential lack of sustainability. Topical plasmids do not cross the corneal epithelial barrier and repeated intrastromal injections are not clinically appealing. To date, gene therapy has also relied on the use of viral vectors for long-term effect. These methods are plagued by virus-induced inflammation, the potential for viral replication and infectiousness, and possible induction of oncogenesis.

An intriguing question is whether long-term suppression of VEGF in the setting of injury, as by nanoparticles, affects biological processes other than angiogenesis. Important areas in the cornea injury model relevant to this question include stromal remodeling, which occurs for weeks after alkali injury,<sup>32,33</sup> and rate of corneal re-epithelialization, which generally occurs over the course of 1 to 2 weeks after alkali injury.<sup>34</sup> VEGF is known to affect leukocyte infiltration and several enzymes involved in stromal remodeling, including collagenase, MMP-2, MMP-9, and MT1-MMP.<sup>33,35–40</sup> However, the role of VEGF in re-epithelialization after alkali injury is not well elucidated. Investigating the effects of long-term VEGF suppression on such processes will also be necessary, to gain a full understanding of the potential and pitfalls of nanoparticle-mediated antiangiogenic intervention. Future research will necessitate characterization of *in vivo* dose-response relationships of nanoparticles expressing plasmids. These studies are under way.

Long-term delivery of antiangiogenic agents is needed in situations in which preemptive intervention would be of benefit (e.g., to prevent postoperative angiogenesis in patients undergoing corneal transplantation) or as a long-term intervention in situations of chronic disease involving angiogenesis (e.g., corneal injury). Compared with existing intraocular therapies, the approach we have outlined in this article has the advantages of being a nonviral, biodegradable platform for long-term control of angiogenesis and of having high specificity and affinity for the target molecule, because receptor subunits are the therapeutic substrate. Therefore, biodegradable albumin nanoparticles may offer the attributes necessary to achieve long-term inhibition and regression of angiogenesis in the cornea, especially when delivered intrastromally.

### Acknowledgments

The authors thank Katsuya Miyake (Imaging Core Facility, Medical College of Georgia), Kimberly Smith (Auxiliary Histopathology Laboratory, Medical College of Georgia), and Tom Bargar (Electron Micro-

copy Core Facility, University of Nebraska Medical Center) for assistance with transmission electron microscopy.

## References

- Epstein RJ, Stulting RD, Hendricks RL, Harris DM. Corneal neovascularization: pathogenesis and inhibition. *Cornea*. 1987;6:250-257.
- Macular Photocoagulation Study Group. Argon laser photocoagulation for neovascular maculopathy; five-year results from randomized clinical trials (published correction appears in *Arch Ophthalmol* 1992;110:761). *Arch Ophthalmol*. 1991;109:1109-1114.
- Census Report 2001*. Washington, DC: U.S. Bureau of the Census; 2001.
- Dvorak HF, Nagy JA, Feng D, Brown LF, Dvorak AM. Vascular permeability factor/vascular endothelial growth factor and the significance of microvascular hyperpermeability in angiogenesis. *Curr Top Microbiol Immunol*. 1999;237:97-132.
- Klein R, Wang Q, Klein BE, Moss SE, Meuer SM. The relationship of age-related maculopathy, cataract, and glaucoma to visual acuity. *Invest Ophthalmol Vis Sci*. 1995;36:182-191.
- Carmeliet P, Collen D. Role of vascular endothelial growth factor and vascular endothelial growth factor receptors in vascular development. *Curr Top Microbiol Immunol*. 1999;237:133-158.
- Neufeld G, Cohen T, Gengrinovitch S, Poltorak Z. Vascular endothelial growth factor (VEGF) and its receptors. *FASEB J*. 1999;13:9-22.
- Shibuya M. Structure and dual function of vascular endothelial growth factor receptor-1 (Flt-1). *Int J Biochem Cell Biol*. 2001;33:409-420.
- Wiesmann C, Fuh G, Christinger HW, Eigenbrot C, Wells JA, de Vos AM. Crystal structure at 1.7 Å resolution of VEGF in complex with domain 2 of the Flt-1 receptor. *Cell*. 1997;91:695-704.
- Bellamy WT, Richter L, Sirjani D, et al. Vascular endothelial cell growth factor is an autocrine promoter of abnormal localized immature myeloid precursors and leukemia progenitor formation in myelodysplastic syndromes. *Blood*. 2001;97:1427-1434.
- Casella I, Feccia T, Chelucci C, et al. Autocrine-paracrine VEGF loops potentiate the maturation of megakaryocytic precursors through Flt1 receptor. *Blood*. 2003;101:1316-1323.
- Fiedler W, Graeven U, Ergun S, et al. Vascular endothelial growth factor, a possible paracrine growth factor in human acute myeloid leukemia. *Blood*. 1997;89:1870-1875.
- Gerber HP, Malik AK, Solar GP, et al. VEGF regulates haematopoietic stem cell survival by an internal autocrine loop mechanism. *Nature*. 2002;417:954-958.
- Pelham HR. The retention signal for soluble proteins of the endoplasmic reticulum. *Trends Biochem Sci*. 1990;15:483-486.
- Shvartsman SY, Hagan MP, Yacoub A, Dent P, Wiley HS, Lauffenburger DA. Autocrine loops with positive feedback enable context-dependent cell signaling. *Am J Physiol*. 2002;282:C545-C559.
- Barleon B, Sozzani S, Zhou D, Weich HA, Mantovani A, Marme D. Migration of human monocytes in response to vascular endothelial growth factor (VEGF) is mediated via the VEGF receptor flt-1. *Blood*. 1996;87:3336-3343.
- Barleon B, Totzke F, Herzog C, et al. Mapping of the sites for ligand binding and receptor dimerization at the extracellular domain of the vascular endothelial growth factor receptor FLT-1. *J Biol Chem*. 1997;272:10382-10388.
- Browder TM, Dunbar CE, Nienhuis AW. Private and public autocrine loops in neoplastic cells. *Cancer Cells*. 1989;1:9-17.
- Chen JD, Bai X, Yang AG, Cong Y, Chen SY. Inactivation of HIV-1 chemokine co-receptor CXCR-4 by a novel intrakine strategy. *Nat Med*. 1997;3:1110-1116.
- Kreitman RJ, Puri RK, Pastan I. Increased antitumor activity of a circularly permuted interleukin 4-toxin in mice with interleukin 4 receptor-bearing human carcinoma. *Cancer Res*. 1995;55:3357-3363.
- Luis Abad J, Gonzalez MA, del Real G, et al. Novel interfering bifunctional molecules against the CCR5 coreceptor are efficient inhibitors of HIV-1 infection. *Mol Ther*. 2003;8:475-484.
- Aukunuru JV, Ayalasomayajula SP, Kompella UB. Nanoparticle formulation enhances the delivery and activity of a vascular endothelial growth factor antisense oligonucleotide in human retinal pigment epithelial cells. *J Pharm Pharmacol*. 2003;55:1199-1206.
- Kompella UB, Bandi N, Ayalasomayajula SP. Subconjunctival nano- and microparticles sustain retinal delivery of budesonide, a corticosteroid capable of inhibiting VEGF expression. *Invest Ophthalmol Vis Sci*. 2003;44:1192-1201.
- Singh N, Amin S, Richter E, et al. Flt-1 intraceptors inhibit hypoxia-induced VEGF expression in vitro and corneal neovascularization in vivo. *Invest Ophthalmol Vis Sci*. 2005;46:1647-1652.
- Merodio M, Irache JM, Valamanesh F, et al. Ocular disposition and tolerance of ganciclovir-loaded albumin nanoparticles after intravitreal injection in rats. *Biomaterials*. 2002;23:1587-1594.
- Stechschulte SU, Jousseaume AM, von Recum HA, et al. Rapid ocular angiogenic control via naked DNA delivery to cornea. *Invest Ophthalmol Vis Sci*. 2001;42:1975-1979.
- Proia AD, Chandler DB, Haynes WL, et al. Quantitation of corneal neovascularization using computerized image analysis. *Lab Invest*. 1988;58:473-479.
- Ambati BK, Jousseaume AM, Ambati J, et al. Angiostatin inhibits and regresses corneal neovascularization. *Arch Ophthalmol*. 2002;120:1063-1068.
- Amano S, Rohan R, Kuroki M, Tolentino M, Adamis AP. Requirement for vascular endothelial growth factor in wound- and inflammation-related corneal neovascularization. *Invest Ophthalmol Vis Sci*. 1998;39:18-22.
- Ambati BK, Anand A, Jousseaume AM, Kuziel WA, Adamis AP, Ambati J. Sustained inhibition of corneal neovascularization by genetic ablation of CCR5. *Invest Ophthalmol Vis Sci*. 2003;44:590-593.
- Ambati BK, Jousseaume AM, Kuziel WA, Adamis AP, Ambati J. Inhibition of corneal neovascularization by genetic ablation of CCR2. *Cornea*. 2003;22:465-467.
- Katakami C, Fujisawa K, Sahori A, et al. Localization of collagen (I) and collagenase mRNA by in situ hybridization during corneal wound healing after epikeratophakia or alkali-burn. *Jpn J Ophthalmol*. 1992;36:10-22.
- Shimoda M, Ishizaki M, Saiga T, Yamanaka N. Expression of matrix metalloproteinases and tissue inhibitor of metalloproteinase by myofibroblasts-morphological study on corneal wound healing (in Japanese). *Nippon Ganka Gakkai Zasshi*. 1997;101:371-379.
- Sosne G, Szliter EA, Barrett R, Kernacki KA, Kleinman H, Hazlett LD. Thymosin beta 4 promotes corneal wound healing and decreases inflammation in vivo following alkali injury. *Exp Eye Res*. 2002;74:293-299.
- Burbridge MF, Coge F, Galizzi JP, Boutin JA, West DC, Tucker GC. The role of the matrix metalloproteinases during in vitro vessel formation. *Angiogenesis*. 2002;5:215-226.
- Gan L, Fagerholm P, Palmblad J. Vascular endothelial growth factor (VEGF) and its receptor VEGFR-2 in the regulation of corneal neovascularization and wound healing. *Acta Ophthalmol Scand*. 2004;82:557-563.
- Owen JL, Iragavarapu-Charyulu V, Gunja-Smith Z, Herbert LM, Grosso JF, Lopez DM. Up-regulation of matrix metalloproteinase-9 in T lymphocytes of mammary tumor bearers: role of vascular endothelial growth factor. *J Immunol*. 2003;171:4340-4351.
- Wang H, Keiser JA. Vascular endothelial growth factor upregulates the expression of matrix metalloproteinases in vascular smooth muscle cells: role of flt-1. *Circ Res*. 1998;83:832-840.
- Wang H, Olszewski B, Rosebury W, Wang D, Robertson A, Keiser JA. Impaired angiogenesis in SHR is associated with decreased KDR and MT1-MMP expression. *Biochem Biophys Res Commun*. 2004;315:363-368.
- Zhang H, Li C, Baciu PC. Expression of integrins and MMPs during alkaline-burn-induced corneal angiogenesis. *Invest Ophthalmol Vis Sci*. 2002;43:955-962.